

## STUDY OF IMPEDANCES AND INSTABILITIES IN J-PARC

Takeshi Toyama, Kazuhito Ohmi, KEK, Oho 1-1, Tsukuba, Ibaraki, Japan  
 Yoshihiro Shobuda, JAERI, Tokai-Mura, Naka-Gun, Ibaraki, Japan

### Abstract

Two high intensity proton synchrotrons with energies of 3 GeV and 50 GeV are planned in J-PARC. Longitudinal impedances and instabilities, which are caused by beam chamber, cavities, kicker magnets and others, are mainly discussed in this paper.

### INTRODUCTION

J-PARC (Japan Proton Accelerator Research Complex) project comprises a 600 MeV linac, a 3 GeV rapid-cycling synchrotron (RCS), and a 50 GeV synchrotron (MR) [1]. A half of the 400 MeV beams from the linac are injected to the RCS. The RCS accelerates two bunches of  $4.15 \times 10^{13}$  protons and the MR eight (fifteen, in phase I) bunches of  $4.13 \times 10^{13}$  ( $2.2 \times 10^{13}$ ) protons. Many elements will be installed in the rings, which might cause the beam unstable via coupling impedances. Impedance estimates with some formulae and/or a coaxial wire method are obtained for RF cavities, kicker magnets, vacuum chambers, and vacuum components. The stability criteria were applied for these impedances. The report will focus on the RCS. The acceleration cycle of the RCS is 25 Hz. Therefore special care is necessary for vacuum pipes in magnets.

### COAXIAL WIRE MEASUREMENTS

A tin coated copper (or copper) wire of 0.4 mm diameter (or 0.2 mm diameter) was stretched in the device under test with appropriate resistors for matching to 50  $\Omega$  cables at both ends [2]. Network analyzer (hp 8753E) was connected to measure the S21, transmission coefficient.

#### RF cavity

Eleven RF cavities will be installed at one of three insertion sections in the RCS [3]. The wire measurement was performed for a prototype system consisting of three rf cavities connected in series which will be utilized for the MR. The parameters are similar to the RCS one. Looking from the power supply the circuit is connected in parallel as shown in Fig. 1. The transmission coefficient for a dummy pipe, same in length and diameter as the RF cavity system, was used as a reference,  $S_{21}^{REF}$ . The transmission coefficient was converted to the coupling impedance with the standard log formula [2]

$$Z_L = -2Z_c \ln \left[ \frac{S_{21}^{DUT}}{S_{21}^{REF}} \right].$$

The results for parasitic modes are summarized in Table 1.

**Table 1:** Parasitic modes of the RF cavity

f (MHz)	Q	R <sub>sh</sub> ( $\Omega$ )
5.1	40	6
18.1	250	5.5
18.4	300	70
30.8	150	15
31.5	200	11
364	20	450
385	80	2800
416	30	350

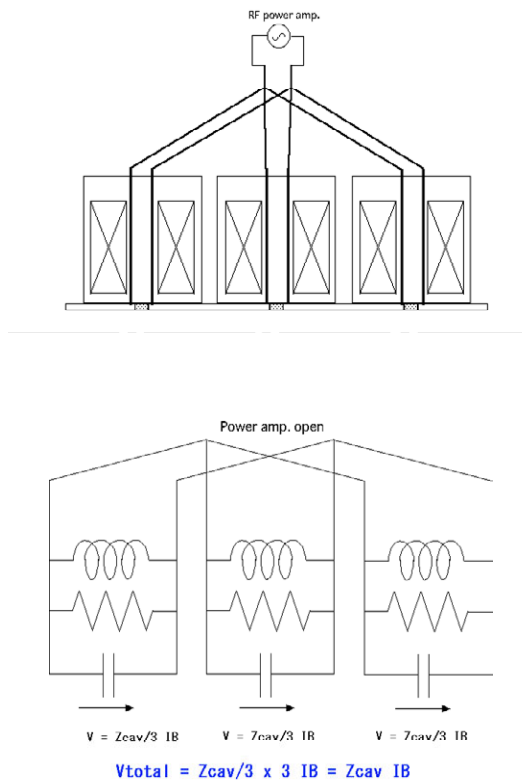


Figure 1: Measurement setup of the RF cavity.

The parasitic resonance at  $f = 385$  MHz is related with the gap capacitors. Four vacuum capacitors (400 pF x4) per acceleration gap (ceramic break) will be mounted in the original design for the MR. For the RCS the capacitance will be 200-400 pF per gap and the inner diameter 247 mm. Alignment of the capacitors and the type of capacitors (small ceramic capacitors) affected the characteristics of the resonance. Figure 2 shows impedance variation with a different number of capacitors. The red, magenta, blue and black lines correspond to four, three, two and one capacitor(s). This fact suggests that these are capacitor related resonances. Though the actual RCS cavities will have a little different parameter, a similar resonance may appear and need mitigation.

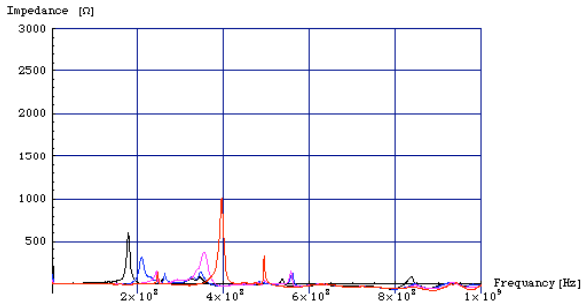


Figure 2: RF cavity resonances with different number of capacitors. The real part of the impedances is shown.

**Kicker magnet**

Five and three kicker magnets will be installed in two neighbouring cells of the extraction insertion. The circuit diagram of the proto-type kicker is shown in Fig. 3 [4].

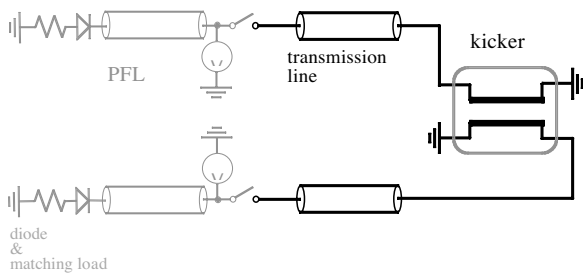


Figure 3: Circuit diagram of the kicker magnet.

The 500 mm length dummy rectangular ducts fitting to the kicker aperture were attached to the kicker end plate. The wire was stretched in the duct and the kicker itself. The coaxial cable length from thyratrons to the kicker corresponds to a delay of 774 ns. This produces multiple reflections in  $Z_L$  as observed in Fig. 4.

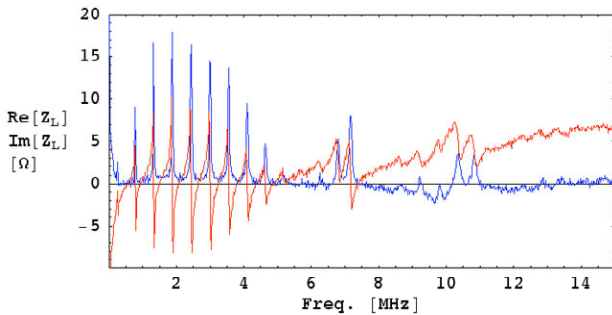


Figure 4: Impedance of the kicker. Blue line: real part, red line: imaginary part.

**VACUUM CHAMBER**

Vacuum chamber comprises titanium (or stainless steel) pipes at field free regions and RF-shielded ceramic pipes

in dipole and quadrupole magnets due to rapid field variation (25 Hz). Table 2 shows details of the vacuum chambers of the RCS.

**Table 2: RCS vacuum chambers**

Type	Inner diameter (mm)	Length (m)
Ti or SUS	~250 - ~330	~160
RF shielded ceramic	~260 - ~380	~190

Design principle of the RF shielded ceramic pipe is: shielding the electromagnetic fields produced by the beam, compromising the shielding efficiency and eddy current loss, and simplifying production and maintenance process.

The copper stripes of ~0.5 mm in thickness and 5 mm in width are electro-formed on the outer surface of the pipe [5]. The inner surface of the pipes will be coated with TiN of 10 - 15 nm in thickness to suppress secondary electron emission. At one end of the pipe, there will be cuts of the stripes and ceramic capacitors of ~300 nF per each stripe will be attached to prevent the eddy current induced by the magnets.

Electromagnetic waves produced by the beam in two-dimensional boundary have been calculated with simplified geometry [6]. The resistances of the TiN coating and RF shield are included in the calculation. The results with the fraction of the shielding area, 50 %, and the length  $L = 348$  m are shown in Fig. 6 and 7. The space charge impedance is dominating.

**RF shield**

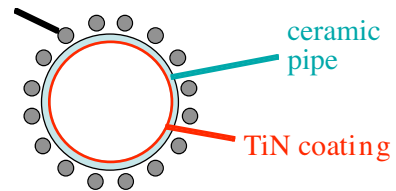


Figure 5: 2D model of the RF shielded ceramic pipe.

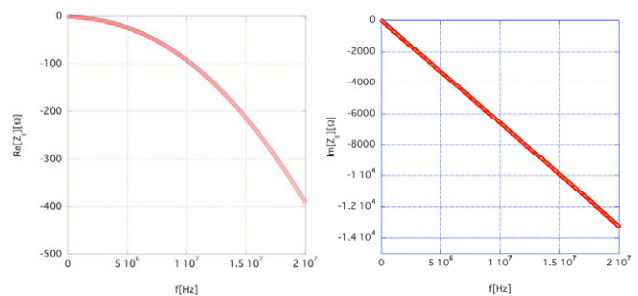


Figure 6:  $Z_L$  of the RF shielded ceramic pipe (400 MeV).  $Re[Z] < 0$  corresponds to deceleration.

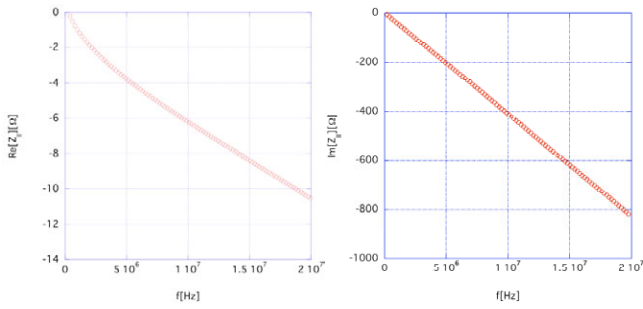


Figure 7:  $Z_L$  of the RF shielded ceramic pipe (3 GeV).  $\text{Re}[Z] < 0$  corresponds to deceleration.

**Pumping ports**

Using an analytical expression for a circular hole of radius  $h \sim 130$  mm on a vacuum pipe of radius  $b \sim h$ ,

$$\frac{Z_L}{n} = j \omega_0 \frac{Z_0}{6\pi^2} \frac{h^3}{cb^2},$$

the impedance is estimated as  $Z_L/n \sim j 0.017 \Omega/\text{port}$ . This can be reduced to  $\sim j 0.0004 \Omega/\text{port}$  with a metal mesh. The number of the pumping ports will be  $\sim 50$ . Total impedance will, therefore, amount to  $\sim j 0.02 \Omega$ .

**Pipe transitions**

There will be transition regions between the vacuum chambers in the dipole and quadrupole magnets due to size differences. Model calculation using cylindrical transition from 125 mm to 190 mm within a distance of 140 mm (25 degree taper) shows  $\sim j 0.013 \Omega/\text{transition}$ .

**Collimators**

Using an analytical expression

$$\frac{Z_L}{n} = j \frac{Z_0 h^2}{2\pi^2 b R} \left( 2 \ln \left( \frac{2\pi b}{h} \right) + 1 \right) / 2,$$

where  $b=0.07$  m the vacuum pipe radius,  $h=0.028$  m the collimator height and  $R \sim 50$  m the RCS radius, the impedance is  $j 14$  m $\Omega/\text{collimator}$ .

Table 3: Longitudinal Impedances in the RCS

	$ Z_L / n  (\Omega)$
RF cavity	( $\sim 17$ )
Kicker	$\sim 70$
Ceramic pipe	$\sim 1000$ (400 MeV)
Pumping port	0.02
Pipe transition	0.14
Collimator	1.3

**STABILITY ESTIMATES**

Keil-Schnell-Boussard (KSB) criteria are calculated with the RCS machine parameters in Table 3. The particle distribution in the bunch affects the results. Here the distribution  $\sin(\pi z/l_B)$ . It should be noticed that the KSB

criteria is applicable to the instabilities growing faster than the synchrotron oscillation and that in high Q resonators the wake fields might continue longer than the bunch length in which case the impedance Z should be replaced by  $Z_{\text{eff}} = Z Q_{\text{eff}}/Q$ ,  $Q_{\text{eff}} = \omega_r \sigma_z/v_B$ , where  $\omega_r$  is the resonance frequency,  $\sigma_z$  the rms bunch length and  $v_B$  the speed of the beam. Another stability consideration will be presented elsewhere. In the case of the RF cavity,  $Q_{\text{eff}} \sim Q$  and  $Z_{\text{eff}} \sim Z$ . The kicker resonances are very low and  $Q_{\text{eff}} < Q/10$ , then the effect may be small as far as KBS criteria concerned. Though the RF shielded ceramic pipe has large capacitive impedance, the impedance is less than the threshold.

Table 4: Keil-Schnell-Boussard criteria for the RCS

Symbol	Inj. (181MeV)	Inj. (400MeV)	Ext.
L (m)	348.3	348.3	348.3
$\gamma$	1.2	1.4	4.2
$N_p$ ( $\times 10^{13}$ )	0.6x4.15	4.15	4.15
$l_B$ (m)	110	110	82
$\Delta p/p$ (%)	0.84	0.85	0.38
$\eta$	-0.69	-0.48	-0.047
$\beta_{x,y}$	8-9	8-9	8-9
$ Z_L/n _{\text{th}} (\Omega)$	6200	3100	140
$ Z_T/n _{\text{th}} (\text{k}\Omega/\text{m})$	200-210	98-100	9.6-10

**SUMMARY**

Coupling impedances are measured or calculated for the J-PARC 3 GeV RCS. Further impedance evaluation is needed including  $Z_T$ 's and other equipments.

Beam stability criteria were also obtained using KSB formula. The longitudinal impedance of the RCS is less than the stability threshold. Further stability consideration is in progress.

The authors thank the RF and kicker group members for measuring and evaluating the impedances of the devices.

**REFERENCES**

- [1] Y. Yamazaki, Accelerator Technical Design Report for J-PARC, KEK Report 2002-13, JAERI-Tech 20003-044.
- [2] F. Caspers, in Handbook of Accelerator Physics and Engineering, ed. A. W. Chao and M. Tigner (1999).
- [3] M. Yoshii et al., Proc. of EPAC2002, 2182.
- [4] E. Nakamura, et al., Proc. of the 14th Symp. on Accel. Science and Technology (2003, in Japanese).
- [5] M. Kinsho et al., J. Vac. Sci. Technol. A20 (3), (2002) p.829.
- [6] T.-S. F. Wang et al., Phys. Rev. ST Accel. Beams 4, 104201 (2001). Y. Shobuda, in preparation.